Single equation without inequalities to represent a composite curve

E. Chicurel-Uziel

Instituto de Ingeniería, Universidad Nacional Autónoma de México, Apdo. Postal 70-472, Coyoacan 04510, Mexico

Abstract

A scheme is proposed based on an extension of Analytic Geometry to represent a composite curve either with a single equation or with two equations in the case of parametric representation, or three equations in the case of parametric representation of 3D surfaces, without the use of inequalities and valid from minus infinity to plus infinity. The general equations of the regular polygon, the polygonal cylinder as well as the equation of the main view of the chain sprocket are established.
© 2003 Elsevier B.V. All rights reserved.

Keywords: Polygon equation; Sprocket equation; Finite segment Analytic Geometry; Composite curve equation; Concatenated curve

1. Introduction

In the last few decades a new discipline known as Computational Geometry has arisen, which, among other problems, deals with intersections of line segments and polygons and has been applied mainly to Computer Graphics, Robotics, Geography and CAD/CAM (De Berg et al., 1998, pp. 1941; Preparata and Shamos, 1985; Hakimi and Schmeichel, 1991; Milenkovic, 1993) and even to roadway geometry to determine its current condition (Drakopoulos and Örnek, 2000). Since Computational Geometry is based on Computer Science, particularly in Algorithmics, it has a great potential, but its use requires, at least, a basic knowledge of these disciplines.

This paper also refers to the handling of finite line and curve segments, polygons and composite curves as well as their intersections, but by different means, namely, an extension of Analytic Geometry which makes use of conventional algebraic and transcendental functions so its application requires little or no knowledge of either Computer Science or Algorithmics. Many problems require no more than a hand-held graphics calculator. Resorting to a symbolic computer language such as *Mathematica, Maple or Matlab* permits to take full advantage of this methodology, but only to handle analytical

---

E-mail address: ecu@pumas.iingen.unam.mx (E. Chicurel-Uziel).

expressions which often involve a considerable amount of computations. The user does not need to do any programming.

Most of the mathematical devices that comprise the previously mentioned extension of Analytic Geometry were proposed in Cartesian form (Chicurel-Uziel, 1999/2000, 2000, 2001a, 2001b), some of them are presented in the present paper adapted to polar or parametric forms. In (Chicurel-Uziel, 1999/2000) a pure algebraic equation to represent the Heaviside unit step function, which does not require any inequalities, was proposed. Also in (Chicurel-Uziel, 1999/2000) a concatenation procedure for linking curve segments was proposed to facilitate the use in the computer of the Clebsch Method for beam deflections. The periodizer and alternator functions introduced in (Chicurel-Uziel, 2000) make possible the non-series, no transform, exact representation of periodic, non-harmonic, continuous or discontinuous functions, and the reflect and repeat function introduced in (Chicurel-Uziel, 2001a) further facilitates the representation of a large class of such functions. References (Chicurel-Uziel, 2000, 2001a, 2001b) illustrate the application of both the concatenation procedure and these special functions in vibration problems.

As mentioned in the previous paragraph, this approach has been applied to engineering problems. The purpose of the present work is to explore the possibilities resulting from the use of these techniques in Analytic Geometry. This scheme permits the representation of composite curves in a manner similar to the conventional manner used for the representation of plain, non-composite curves. A single Cartesian equation may represent a single-valued, plane, composite curve which may be of finite or infinite length. A multi-valued plane composite curve, open or closed, with or without polar symmetry, may be represented either by a single polar equation or by two parametric equations. Three parametric equations suffice for the representation of composite 3D surfaces. In no case are inequalities required. This capability leads to the establishment of the general equation of the polygon as well as that of the chain sprocket.

2. Mathematical devices

2.1. A useful representation of the Heaviside unit step function

The following representations of three well known functions were proposed in (Chicurel-Uziel, 1999/2000):

Absolute Value or "V" function:

$$V(x,a) = |x - a| = \sqrt{(x-a)^2}. \tag{1}$$

"Jump" or Relay function:

$$J(x,a) = \frac{V(x,a)}{(x-a)} = \frac{(x-a)}{V(x,a)}. \tag{2}$$

Heaviside unit step function, Fig. 1(a):
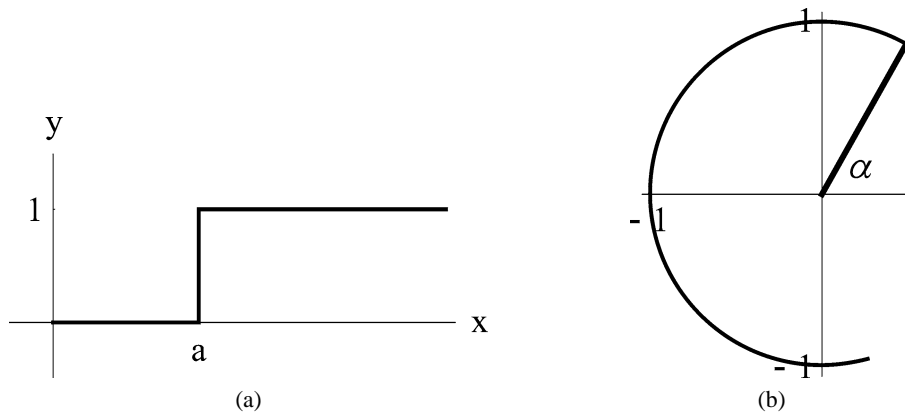
$$H(x,a) = \frac{1}{2}\{1 + J(x,a)\}. \tag{3}$$

Fig. 1. Heaviside unit step function: (a) Cartesian version, plot of Eq. (3). (b) Polar version, plot of Eq. (4).

Notice that these are self contained, single equation representations that do not require any inequalities and, furthermore, they are valid from $x = -\infty$ to $x = +\infty$. The following is a polar version of the Heaviside unit step function, Fig. 1(b):

$$H(\theta, \alpha) = \frac{1}{2}\{1 + J(\theta, \alpha)\}. \tag{4}$$

2.2. Equation of a finite curve segment

The Heaviside unit step function may be used as a "switch", i.e., a function may be switched on when multiplied by its positive value and switched off when multiplied by its negative value. So that the finite segment of the curve $f(x)$ from $x = a$ to $x = b$ is represented as:

$$g(x) = f(x)\{H(x, a) - H(x, b)\}. \tag{5}$$

2.3. Concatenation procedure

Eq. (5) leads immediately to the concatenation procedure (Chicurel-Uziel, 1999/2000, 2000, 2001a, 2001b). A composite function:

$$
\begin{aligned}
f(x) &= f_{12}(x), & a_1 \leqslant x \leqslant a_2, \\
f(x) &= f_{23}(x), & a_2 \leqslant x \leqslant a_3, \\
f(x) &= f_{34}(x), & a_3 \leqslant x \leqslant a_4, \\
&\ \ \vdots & \vdots \\
f(x) &= f_{n-1,n}(x), & a_{n-1} \leqslant x \leqslant a_n,
\end{aligned}
$$

may be expressed as:

$$f(x) = f_{12}(x) + H(x, a_2)\big(-f_{12}(x) + f_{23}(x)\big) + H(x, a_3)\big(-f_{23}(x) + f_{34}(x)\big) + \cdots$$
$$+ H(x, a_{n-1})\big(-f_{n-2,n-1}(x) + f_{n-1,n}(x)\big), \quad a_1 \leqslant x \leqslant a_n, \tag{6}$$
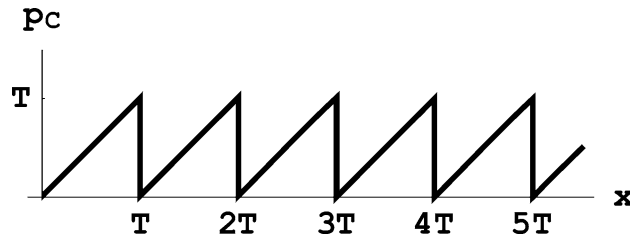
Fig. 2. Cartesian periodizer function, plot of Eq. (8).

or as the single equation:

$$f(x) = H(x, a_1) f_{12}(x) + H(x, a_2)\big(-f_{12}(x) + f_{23}(x)\big) + H(x, a_3)\big(-f_{23}(x) + f_{34}(x)\big) + \cdots$$
$$+ H(x, a_{n-1})\big(-f_{n-2,n-1}(x) + f_{n-1,n}(x)\big) + H(x, a_n)\big(-f_{n-1,n}(x)\big). \tag{7}$$

Clearly (7) is valid from $x = -\infty$ to $x = +\infty$.

2.4. Cartesian periodizer function

This function was introduced in (Chicurel-Uziel, 2000) and is represented by the following equation, Fig. 2:

$$p_C(x, T) = \frac{T}{2} - \frac{T}{\pi} \arctan\left(\cot \frac{\pi}{T} x\right). \tag{8}$$

If in a function $f(x)$, x is replaced by p_C the resulting function is the segment of $f(x)$ contained in the interval $0 \leqslant x \leqslant T$ repeated indefinitely.

2.5. Polar periodizer function

Replacing x by $(\theta - \theta_0)$ and T by $2\pi/N$ in (8) results in the polar periodizer function, introduced in this paper and adapted for use in connection with figures with polar symmetry and a whole number of lobes N, Fig. 3:

$$p(\theta, N, \theta_0) = \frac{\pi}{N} - \frac{2}{N} \arctan\left[\cot\left\{\frac{N(\theta - \theta_0)}{2}\right\}\right]. \tag{9}$$

Fig. 3 illustrates (9) for $N = 5$ and $\theta_0 = 0$.

If in a function $f(\theta)$, θ is replaced by $p(\theta, N, 0)$ the resulting function $f(p(\theta, N, 0))$ is made up of the initial segment of $f(\theta)$ from $\theta = 0$ to $\theta = T$ repeated N times in the interval $0 \leqslant \theta \leqslant 2\pi$. The function $f(p(\theta, N, \theta_0))$ is identical to the function $f(p(\theta, N, 0))$ except that the former is rotated an angle θ_0 counter-clockwise with respect to the latter.

2.6. Stairs function

The single equation to represent the stairs function S, Fig. 4, which is introduced in this paper, may be derived from the Cartesian periodizer function in the following manner. Consider the straight line:
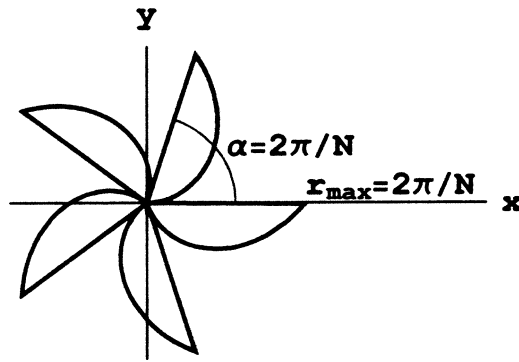
$$y = mx + b. \tag{10}$$

Fig. 3. Polar periodizer function, plot of Eq. (9) for $N = 5$ and $\theta_0 = 0$.
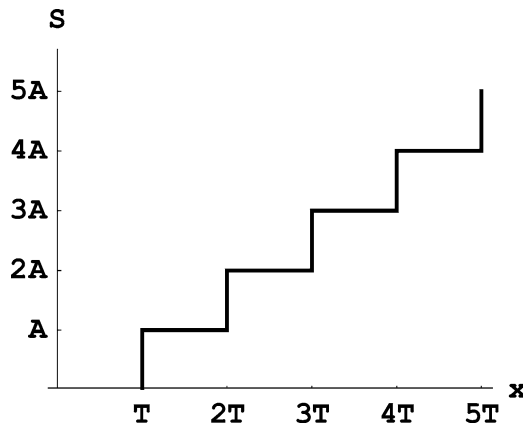

Fig. 4. Stairs function, plot of Eq. (18).

Suppose that S may be obtained thus:

$$S = p_C k + y, \quad k = \text{a constant.} \tag{11}$$

Substituting (10) into (11):

$$S = p_C k + mx + b \tag{12}$$

m, b and k are to be determined. In order to simplify the procedure we consider the pseudo-stairs function S' (a single step) as well as the pseudo-Cartesian periodizer function p'_C (a single lobe of p_C), Fig. 5.

$$S' = AH(x, T), \tag{13}$$
$$p'_C = x - TH(x, T). \tag{14}$$

Notice that $S' = S$ and $p'_C = p_C$ in the interval $0 \leqslant x < 2T$, Fig. 5. Thus we now have the simpler problem, i.e., to determine m, b and k such that:

$$S' = p'_C k + mx + b, \quad 0 \leqslant x < 2T. \tag{15}$$

Substituting (13) and (14) into (15):

$$AH(x, T) = -kTH(x, T) + (k + m)x + b, \quad 0 \leqslant x < 2T, \tag{16}$$
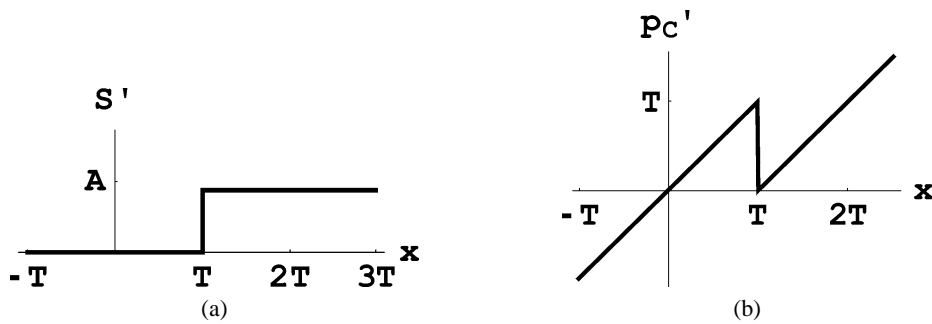
Fig. 5. (a) Pseudo-stairs function (a single step), plot of Eq. (13). (b) Pseudo-Cartesian periodizer function (a single lobe of the periodizer function), plot of Eq. (14).
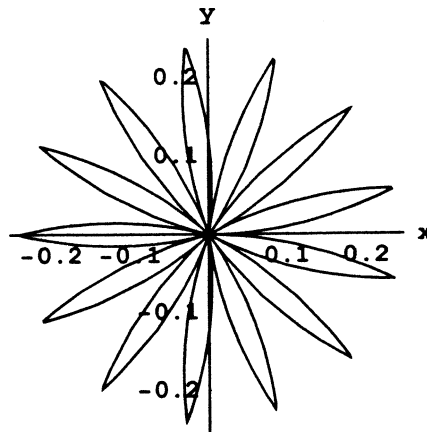

Fig. 6. Polar reflecting and repeating function, plot of Eq. (21) for $N = 13$.

consequently:

$$k = -\frac{A}{T}, \qquad m = \frac{A}{T}, \qquad b = 0 \tag{17}$$

substituting (17) and (8) into (12) yields the stairs function, Fig. 4:

$$S(x, A, T) = A\left\{ -\frac{1}{2} + \frac{x}{T} + \frac{1}{\pi} \arctan\left(\cot \frac{\pi}{T} x \right) \right\}, \tag{18}$$

where A is the magnitude of the riser (vertical distance between consecutive steps) and T is the tread or width of a single step (horizontal distance between two consecutive risers). For an application of this function see Example 4.1.3.

2.7. Polar reflecting and repeating function

The following is the polar version of the reflecting and repeating function introduced in (Chicurel-Uziel, 2001a), Fig. 6:

$$R(\theta, T) = \frac{T}{2\pi} \arccos\left(\cos \frac{2\pi}{T} \theta \right). \tag{19}$$

To use Eq. (19) in connection with a figure with polar symmetry it is convenient to express the period T as a function of the number of lobes:

$$T = \frac{2\pi}{N}. \tag{20}$$

Substituting Eq. (20) into (19) yields:

$$R(\theta, N) = \frac{1}{N} \arccos(\cos N\theta). \tag{21}$$

Fig. 6 is a direct plot of (21) for $N = 13$.

If in a function $f(\theta)$, θ is replaced by $R(\theta, N)$ the resulting function $f(R(\theta, N))$ is made up of N identical lobes in the interval $0 \leqslant \theta \leqslant 2\pi$. The first lobe is made up of two symmetrical halves, i.e., the first half is identical to the initial segment of $f(\theta)$ from $\theta = 0$ to $\theta = T/2$, and the second half is the reflection of the first half with respect to the radius at $\theta = T/2$.

3. Non-symmetrical closed composite figures

3.1. Irregular polygon

The parametric equations of the irregular polygon will now be established. Let the polygon vertices be $P_0(x_0, y_0)$, $P_1(x_1, y_1)$, $P_2(x_2, y_2)$, ..., $P_n(x_n, y_n)$. Since a polygon is a closed figure, $P_n = P_0$, $x_n = x_0$ and $y_n = y_0$. Let s be the variable distance along the perimeter of the polygon measured from point P_0 and s_i the specific distance from point P_0 to point P_i:

$$s_i = \sum_{j=1}^{j=i} \sqrt{(x_j - x_{j-1})^2 + (y_j - y_{j-1})^2}, \quad i = 0, 1, 2, \ldots, n. \tag{22}$$

Clearly $s_n \neq s_0$ since $s_0 = 0$ and $s_n =$ the full length of the perimeter of the polygon.

The double subscripted symbols $x_{i,i+1}$ and $y_{i,i+1}$ designate the dependent variables associated with the parametric equations of line segment $\overline{P_i P_{i+1}}$:

$$x_{i,i+1} = \frac{x_{i+1} - x_i}{s_{i+1} - s_i}s + \frac{x_i s_{i+1} - x_{i+1}s_i}{s_{i+1} - s_i},$$
$$y_{i,i+1} = \frac{y_{i+1} - y_i}{s_{i+1} - s_i}s + \frac{y_i s_{i+1} - y_{i+1}s_i}{s_{i+1} - s_i} \tag{23}$$

and in accordance with Eq. (7) the parametric equations of the regular polygon are:

$$x = x_{01} + H(s, s_1)(-x_{01} + x_{12}) + H(s, s_2)(-x_{12} + x_{23}) + \cdots$$
$$\quad + H(s, s_{n-1})(-x_{n-2,n-1} + x_{n-1,n}) + H(s, s_n)(-x_{n-1,n}),$$
$$y = y_{01} + H(s, s_1)(-y_{01} + y_{12}) + H(s, s_2)(-y_{12} + y_{23}) + \cdots \tag{24}$$
$$\quad + H(s, s_{n-1})(-y_{n-2,n-1} + y_{n-1,n}) + H(s, s_n)(-y_{n-1,n}).$$

Since in Eqs. (24) $s \geqslant 0$, it was not necessary to multiply the first term in either one by the unit step $H(s, s_0)$.
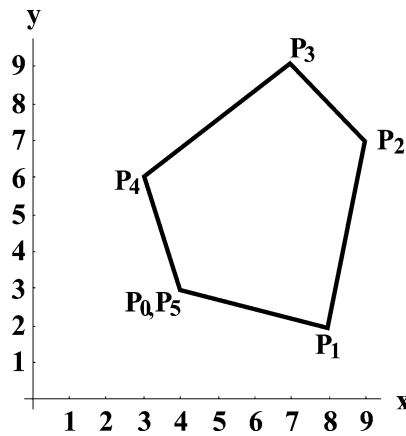
Fig. 7. Irregular polygon, plot of parametric Eqs. (24), Example 3.1.1.

3.1.1. Example. The equation of the irregular pentagon with vertices at points: $P_0(4, 3)$, $P_1(8, 2)$, $P_2(9, 7)$, $P_3(7, 9)$, $P_4(3, 6)$, $P_5(4, 3)$, Fig. 7 will be obtained.

Solution. The distances along the perimeter of the polygon measured from the vertex at P_0 are calculated in accordance with (22):

$$\begin{aligned} s_1 &= 4.1231, & s_2 &= 9.2221, & s_3 &= 12.0506, \\ s_4 &= 17.0506, & s_5 &= 20.2128. \end{aligned} \tag{25}$$

The parametric equations of each of the line segments comprising the pentagon are established in accordance with (23):

$$\begin{aligned} x_{01}(s) &= 0.970s + 4, & y_{01}(s) &= -0.243s + 3, \\ x_{12}(s) &= 0.196s + 7.191, & y_{12}(s) &= 0.981s - 2.043, \\ x_{23}(s) &= -0.707s + 15.521, & y_{23}(s) &= 0.707s + 0.479, \\ x_{34}(s) &= -0.8s + 16.640, & y_{34}(s) &= -0.6s + 16.230, \\ x_{45}(s) &= 0.316s - 2.392, & y_{45}(s) &= -0.949s + 22.176. \end{aligned} \tag{26}$$

The parametric equations of this irregular pentagon are obtained substituting $n = 5$ as well as values (25) and Eqs. (26) into Eqs. (24). Fig. 7 is a direct plot of the resulting two parametric equations.

3.1.2. Example (*Non-symmetric figure composed of various curves*). The equation of the curve, shown in Fig. 8 will be obtained. It is composed of the following three segments:

- Circle: $x^2 + y^2 = 4$ from point $P_1(4, 0)$ to point $P_2(0, 4)$.
- Straight line: $y = 2x + 4$ from point $P_2(0, 4)$ to point $P_3(-5, -6)$.
- Parabola: $y = -2\sqrt{4 - x}$ from point $P_3(-5, -6)$ to point $P_1(4, 0)$.

The corresponding polar equations and end points are:

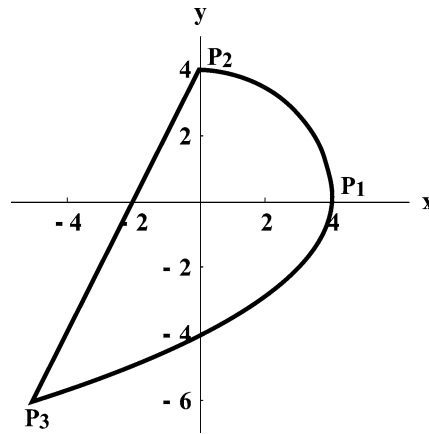- Circle: $r_{12} = 4$ from point $P_1(4, 0)$ to point $P_2(4, \pi/2)$.

Fig. 8. Closed composite curve, plot of Eq. (27).

– Straight line: $r_{23} = \frac{4}{\sin\theta - 2\cos\theta}$ from point $P_2(4, \pi/2)$ to point $P_3(7.81025, 4.01765)$.

– Parabola: $r_{31} = \frac{-2\cos\theta + 2\sqrt{\cos^2\theta + 4\sin^2\theta}}{\sin^2\theta}$ from point $P_3(7.81025, 4.01765)$ to point $P_1(4, 0)$.

The equation of the composite figure is obtained by simply applying the concatenation rule (7):

$$r = r_{12} + H(\theta, 0.5\pi)(-r_{12} + r_{23}) + H(\theta, 4.01765)(-r_{23} + r_{31}) + H(\theta, 2\pi)(-r_{31}). \tag{27}$$

Fig. 8 is a direct plot of (27).

4. Equations of figures with polar symmetry

4.1. Equation of the regular polygon

Consider a polygon of N sides centered at the origin with one vertex lying in the x axis. Consider further the isosceles triangle limited by the x axis, the side of the polygon and the radius of the circumscribed circle drawn from the center of the polygon to the next vertex, Fig. 9. In this triangle:

$$\alpha = \frac{2\pi}{N}, \tag{28}$$

$$\beta = \frac{\pi - \alpha}{2}. \tag{29}$$

Substituting (28) into (29) yields:

$$\beta(N) = \pi\left(\frac{N-2}{2N}\right). \tag{30}$$

The Cartesian equation of the first side (adjacent to the x axis, in the first quadrant) of the polygon is easily established:
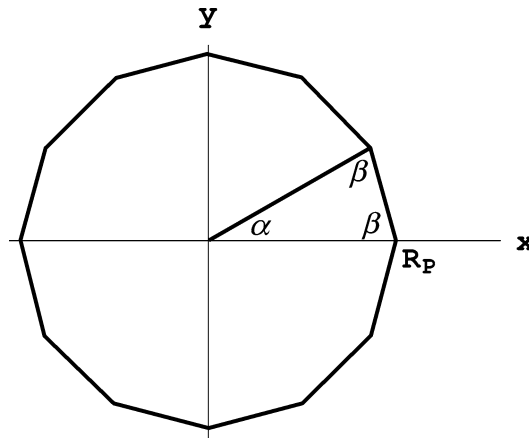
$$y = (R_P - x)\tan\beta. \tag{31}$$

Fig. 9. Regular polygon.

Converting (31) to polar coordinates results in the polar equation of the first side of the polygon:

$$r = \frac{R_P \tan \beta(N)}{\sin \theta + \tan \beta(N) \cos \theta} \tag{32}$$

replacing θ by the periodizer function $p = p(\theta, N, \theta_0)$ yields the polar equation of a regular polygon of N sides, with radius R_P centered at the origin and rotated an angle θ_0:

$$r(\theta, R_P, N, \theta_0) = \frac{R_P \tan \beta(N)}{\sin p(\theta, N, \theta_0) + \tan \beta(N) \cos p(\theta, N, \theta_0)}. \tag{33}$$

Consequently the general parametric equations of a regular polygon of N sides, with radius R, centered at (x_0, y_0) and rotated an angle of θ_0 counter-clockwise follow immediately:

$$x(\theta, R_P, N, \theta_0, x_0) = x_0 + r(\theta, R_P, N, \theta_0) \cos \theta, \tag{34}$$
$$y(\theta, R_P, N, \theta_0, y_0) = y_0 + r(\theta, R_P, N, \theta_0) \sin \theta. \tag{35}$$

4.1.1. Example (*Intersections of a polygon and a parabola*). The two intersections will be determined of a polygon with:

$$N = 11, \qquad R_P = 4, \qquad \theta_0 = 0, \qquad x_0 = 6, \qquad y_0 = 5 \tag{36}$$

and the parabola

$$y_B = \frac{x_B^2}{10}. \tag{37}$$

See Fig. 10.

Solution. Substituting the values (36) into (9), (33), (34) and (35) yields:

$$p = \frac{\pi}{11} - \frac{2}{11} \arctan \left\{ \cot \left(\frac{11}{2} \theta \right) \right\}, \tag{38}$$

$$x_P = 6 + \frac{13.6229 \cos \theta}{\sin p + 3.40573 \cos p}, \tag{39}$$
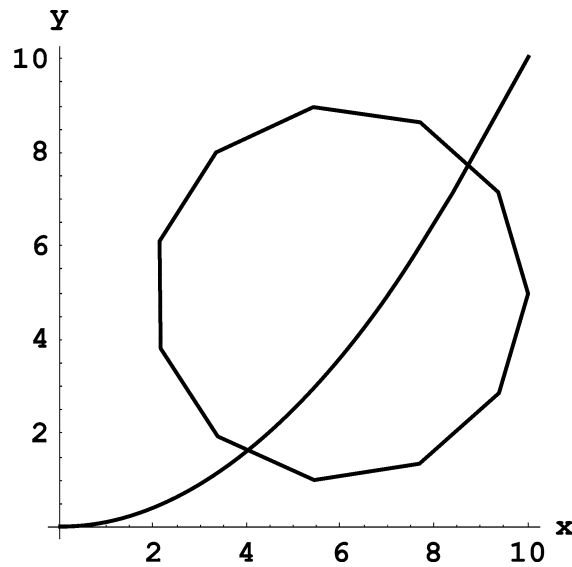
Fig. 10. Superimposed plots of parabola, Eq. (37), and polygon, parametric Eqs. (39) and (40).

$$y_P = 5 + \frac{13.6229 \sin \theta}{\sin p + 3.40573 \cos p}. \tag{40}$$

Relations (39) and (40) are the parametric equations of the specified polygon. At the intersections:

$$x_P = x_B, \qquad y_P = y_B. \tag{41}$$

Since these equations are non-linear they will be substituted by the following:

$$\varepsilon_x = x_P - x_B, \qquad \varepsilon_y = y_P - y_B, \qquad S = \varepsilon_x^2 + \varepsilon_y^2. \tag{42}$$

S was minimized by use of *Mathematica* (Wolfram, 1996) . For the intersection closest to the origin and approximate initial values of $\theta = 5\pi/4$ and $x = 4$ estimated from Fig. 10, the coordinates of the intersection were found to be:

$$\theta = 4.1894, \qquad x = 4.07445, \qquad y = 1.66011 \qquad \left(S = 8.05 \times 10^{-16}\right). \tag{43}$$

For the intersection farthest from the origin and approximate initial values of $\theta = \pi/4$ and $x = 8$, the coordinates of the intersection were found to be:

$$\theta = 0.770257, \qquad x = 8.76498, \qquad y = 7.68249 \qquad \left(S = 3.04 \times 10^{-19}\right). \tag{44}$$

The polygon of Fig. 10 is a direct plot of (39) and (40). Incidentally, Figs. 1–10 may be easily obtained on a hand-held graphics calculator.

4.1.2. Example (*Intersection of a polygonal cylinder with a circular cylinder*). Consider the circular cylinder with a radius $R_C = 2$ and axis along the line: $z = 4 + x/\sqrt{3}$, $y = 0$ as well as the right hexagonal cylinder with a radius $R_P = 2$ and axis along the line: $x = 6$, $y = 0$. The equations for the intersections of these two cylinders, Fig. 11(a), will be determined.
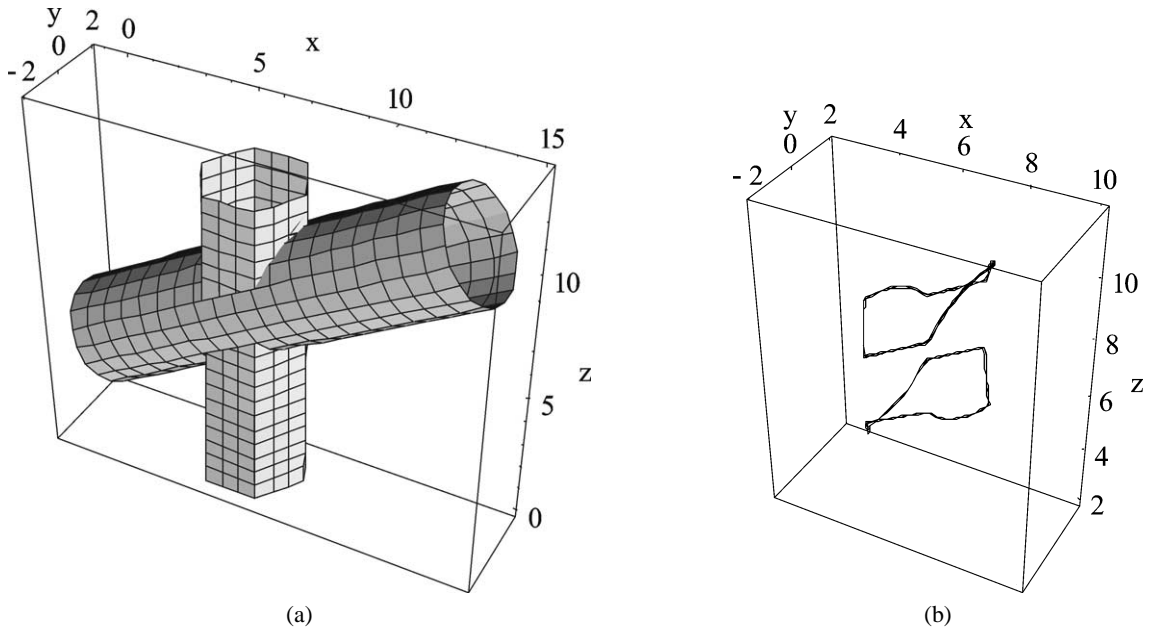
Fig. 11. (a) Superimposed plots of circular cylinder, parametric Eqs. (46), and hexagonal cylinder, parametric Eqs. (52). (b) Intersections of the two cylinders, plot of parametric Eqs. (58).

Using the notation:

ϕ = polar angle of the circular cylinder,

u = axial displacement parameter that generates the surface of the circular cylinder,

γ = angle of rotation of the circular cylinder with respect to the z axis,

z_{C0} = z intercept of the circular cylinder axis.

From the given data:

$$R_C = 2, \qquad z_{C0} = 4, \qquad \gamma = \frac{\pi}{3}. \tag{45}$$

The parametric equations that define the circular cylinder, in terms of the parameters ϕ and u are:

$$\begin{aligned} x_C &= R_C \cos \gamma \cos \phi + u \sin \gamma, \\ y_C &= R_C \sin \phi, \\ z_C &= z_{C0} + u \cos \gamma - R_C \sin \gamma \cos \phi. \end{aligned} \tag{46}$$

Using the notation:

v = axial displacement parameter that generates the surface of the polygonal cylinder,

x_{P0}, y_{P0} = coordinates of the axis of the polygonal cylinder.

From the given data:

$$N = 6, \qquad R_P = 2, \qquad x_{P0} = 6, \qquad y_{P0} = 0, \qquad \theta_0 = 0. \tag{47}$$

Substituting values (47) into (28), (29), (30), (9) and (33) yields:

$$\alpha = \frac{\pi}{3}, \tag{48}$$

$$\beta = \frac{\pi}{3}, \tag{49}$$

$$p(\theta) = \frac{\pi}{6} - \frac{1}{3}\arctan(\cot 3\theta), \tag{50}$$

$$r\big(p(\theta)\big) = \frac{2\sqrt{3}}{\sin p(\theta) + \sqrt{3}\cos p(\theta)}. \tag{51}$$

Using (34) and (35) and introducing the parameter v yields the parametric equations of the polygonal cylinder in terms of the parameters θ and v:

$$\begin{aligned}
x_P(\theta) &= x_{P0} + r\big(p(\theta)\big)\cos\theta, \\
y_P(\theta) &= y_{P0} + r\big(p(\theta)\big)\sin\theta, \\
z_P(v) &= v.
\end{aligned} \tag{52}$$

Fig. 11(a) is the superposition of the direct plot of (52) referring to the hexagonal cylinder and the direct plot of (46) referring to the circular cylinder.

The intersections must comply with the following conditions:

$$x_C = x_P, \qquad y_C = y_P, \qquad z_C = z_P. \tag{53}$$

Substituting (46) and (52) into (53):

$$\begin{aligned}
R_C \cos\gamma \cos\phi + u\sin\gamma &= x_P(\theta), \\
R_C \sin\phi &= y_P(\theta), \\
z_{C0} + u\cos\gamma - R_C \sin\gamma \cos\phi &= v.
\end{aligned} \tag{54}$$

There are four parameters involved in this system of equations, namely: ϕ, θ, u and v. Of these four the most difficult to eliminate is θ thus the other three will be expressed in terms of it:

$$\phi(\theta) = \arcsin\frac{y_P(\theta)}{R_C}, \quad \text{and consequently:} \quad \cos\phi = \pm\frac{\sqrt{R_C^2 - (y_P(\theta))^2}}{R_C}, \tag{55}$$

$$u(\theta) = \frac{x_P(\theta)}{\sin\gamma} \pm \sqrt{R_C^2 - (y_P(\theta))^2}\,\cot\gamma, \tag{56}$$

$$v(\theta) = z_{C0} + x_P(\theta)\cot\gamma \pm \frac{\sqrt{R_C^2 - (y_P(\theta))^2}}{\sin\gamma}. \tag{57}$$

Therefore the parametric equations of the intersections are:

$$\begin{aligned}
x_I(\theta) &= x_{P0} + r\big(p(\theta)\big)\cos\theta, \\
y_I(\theta) &= y_{P0} + r\big(p(\theta)\big)\sin\theta, \\
z_I(\theta) &= z_{C0} + x_I(\theta)\cot\gamma \pm \frac{\sqrt{R_C^2 - (y_I(\theta))^2}}{\sin\gamma}.
\end{aligned} \tag{58}$$

The plus sign of the last equation is associated with the upper intersection while the minus sign is associated with the lower intersection. Fig. 11(b) is a superposition of the direct plots of each of these two systems of equations.

4.1.3. Developable intersections. Example

When intersecting surfaces are developable so are their intersections, of course, and thus their equations may be obtained. The equations of the developed intersections of Example 4.1.2. will be obtained presently. Using the notation:

s_C = distance along the perimeter of the cross section of the circular cylinder,

s_P = distance along the perimeter of the cross section of the polygonal (in this case, hexagonal) cylinder.

The parametric equations of the intersections after developing the surfaces may be represented thus:

$$\left.\begin{array}{l} u = u(\theta) \\ s_C = s_C(\theta) \end{array}\right\} \quad \text{for the circular cylinder,} \tag{59}$$

$$\left.\begin{array}{l} v = v(\theta) \\ s_P = s_P(\theta) \end{array}\right\} \quad \text{for the hexagonal cylinder.} \tag{60}$$

The explicit functional relations are: (56) for $u(\theta)$ and (57) for $v(\theta)$. The explicit functional relations $s_C(\theta)$ and $s_P(\theta)$ will be established presently. Obviously:

$$s_C(\theta) = R_C \phi(\theta), \tag{61}$$

where the explicit functional relation $\phi(\theta)$ is (55). To establish the explicit relation $s_P(\theta)$ we consider, for the present, only the first side of the polygon, i.e., the one adjacent to the x axis in the first quadrant:

$$s_{P1} = \frac{r(\theta)\sin\theta}{\sin\beta} \tag{62}$$

the relation is the same for each side of the polygon and thus θ must be replaced by the Cartesian periodizer function (8) with $T = \alpha = \pi/3$:

$$p_C(\theta) = \frac{\pi}{6} - \frac{1}{3}\arctan(\cot 3\theta) \tag{63}$$

carrying out the replacement in (62):

$$s_{Pi} = \frac{r(p_C(\theta))\sin p_C(\theta)}{\sin\beta}, \tag{64}$$

where s_{Pi} is measured from the start of each side of the polygon. In other words, s_{Pi} grows from zero until it reaches a, the length of one side of the polygon, and then its value drops to zero and starts growing again until it reaches the end of the next side and again drops to zero and so on.

The length of one side of the polygon is:

$$a = 2R_P \sin\frac{\alpha}{2} = 2. \tag{65}$$

The stairs function (18) with the riser $A = a = 2$ and the tread $T = \alpha = \pi/3$ becomes:

$$S(\theta) = -1 + \frac{6}{\pi}\theta + \frac{2}{\pi}\arctan(\cot 3\theta). \tag{66}$$
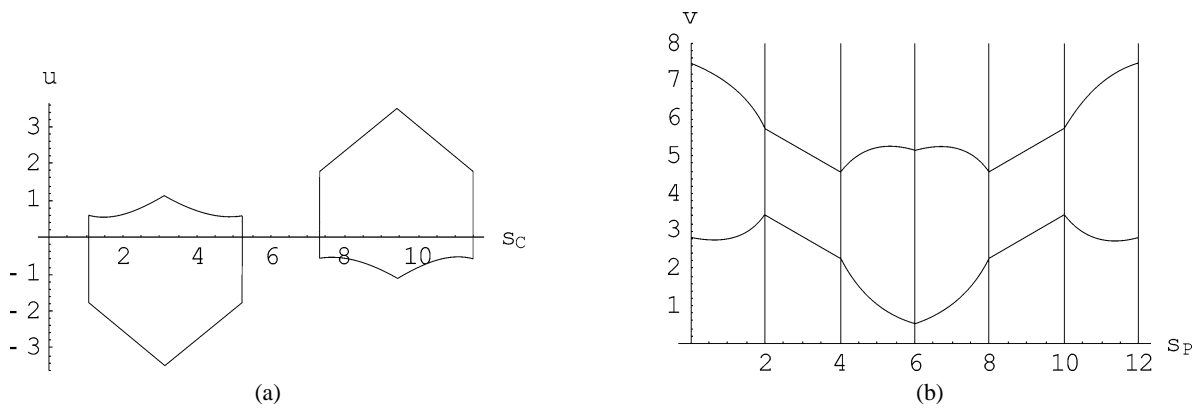
Fig. 12. (a) Developed intersections on the circular cylinder, plot of parametric equations (59). (b) Developed intersections on the hexagonal cylinder, plot of parametric equations (60).

Adding this stairs function to s_{Pi} of Eq. (64) yields

$$s_P(\theta) = s_{Pi}(\theta) + S(\theta),$$ (67)

where s_P is measured from the single starting point $(R_P, 0)$.

Substituting (56) and (61) into (59) yields the explicit parametric equations of the developed intersections in the circular cylinder, the upper intersection resulting from the use of the plus sign of (56) and the lower from the use of the minus sign, Fig. 12(a) is a direct plot of these equations. Likewise substituting (57) and (67) into (60) yields the explicit parametric equations of the developed intersections in the hexagonal cylinder and, here too, the upper intersection results from the use of the plus sign of (57) and the lower from the use of the minus sign. Fig. 12(b) is a direct plot of these equations.

4.2. Derivation of the sprocket equation

The sprocket equation will be established in polar coordinates and it will be made up of the equations of: the toothed contour from $\theta = 0$ to $\theta = 2\pi$, the hub contour from $\theta = 2\pi$ to $\theta = 4\pi$, and the bore and keyway contour from $\theta = 4\pi$ to $\theta = 6\pi$. Once these equations are obtained they will simply be concatenated into a single equation. The following notation will be used:

$D =$ pitch diameter of the sprocket,

$d =$ diameter of the chain roller,

$N =$ number of teeth in the roller,

$P =$ pitch.

4.2.1. Toothed contour

Fig. 13 shows the profile $P_1 P_2 P_3 P_4 P_5$ of one half of a tooth of a roller chain sprocket. The origin of the coordinate system O is not shown but it coincides with the center of the sprocket which lies to the left of the figure, the line OCP_5 is the axis of symmetry of the tooth. The ANSI tooth form is generated by the three circular arcs, $P_1 P_2$, $P_2 P_3$ and $P_4 P_5$ and the straight line segment, $P_3 P_4$ (Oberg et al., 1988). O_1 is the center of the chain roller as well as of the seating curve, arc $P_1 P_2$; R_1 is the radius of the seating
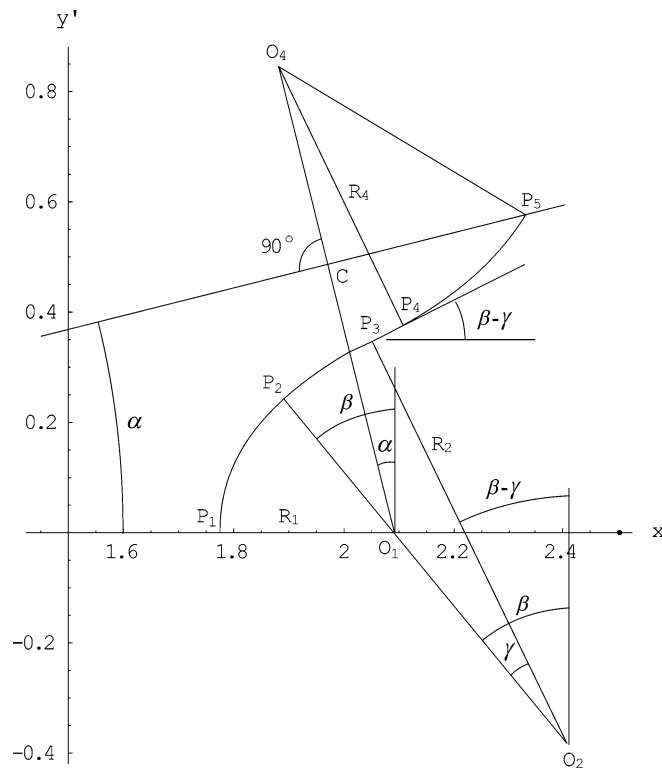
Fig. 13. ANSI tooth form, plot of Eq. (78).

curve; O_2 is the center and R_2 the radius of arc $P_2 P_3$. Straight line segment $P_3 P_4$ is tangent to arc $P_2 P_3$ at point P_3. O_4 is the center and R_4 the radius of arc $P_4 P_5$ which is tangent to the straight line segment $P_3 P_4$ at point P_4. Line $O_1 C O_4$ is the center line of the chain link. The following relations define the dimensions of the tooth as a function of N and d:

$$R_1 = 0.5025d + 0.0015,$$
$$\overline{O_1 O_2} = 0.8d,$$
$$\overline{O_1 O_4} = 1.4d,$$
$$\alpha = \frac{\pi}{N}, \tag{68}$$
$$\beta = \frac{\pi}{180}\left(35 + \frac{60}{N}\right),$$
$$\gamma = \frac{\pi}{180}\left(18 - \frac{56}{N}\right).$$

The distance $\overline{O_1 C}$ in Fig. 13 is equal to one half of the pitch:

$$D = \frac{P}{\sin \alpha}. \tag{69}$$

Referring to Fig. 13

$$x_{01} = \frac{D}{2}, \qquad y_{01} = 0,$$

$$x_{P1} = \frac{1}{2}(D - d), \qquad y_{P1} = 0, \qquad \theta_{P1} = 0,$$

$$x_{02} = \frac{D}{2} + 0.8d \sin\beta, \qquad y_{02} = -0.8d \cos\beta,$$

$$x_{P2} = \frac{D}{2} - R_1 \sin\beta, \qquad y_{P2} = R_1 \cos\beta, \qquad \theta_{P2} = \arctan\frac{y_{P2}}{x_{P2}}, \tag{70}$$

$$R_2 = R_1 + 0.8d,$$

$$x_{P3} = x_{02} - R_2 \sin(\beta - \gamma), \qquad y_{P3} = y_{02} + R_2 \cos(\beta - \gamma), \qquad \theta_{P3} = \arctan\frac{y_{P3}}{x_{P3}},$$

$$x_{04} = 0.5D - 1.4d \sin\alpha, \qquad y_{04} = 1.4d \cos\alpha.$$

P_4 is the intersection of lines $P_3 P_4$ and $O_4 P_4$. The slopes and intercepts of these two lines are, respectively:

$$\begin{aligned} m_a &= \tan(\beta - \gamma), & b_a &= y_{P3} - m_a x_{P3}, \\ m_b &= \tan(\beta - \gamma + 0.5\pi), & b_b &= y_{04} - m_b x_{04}. \end{aligned} \tag{71}$$

The coordinates of P_4 are:

$$x_{P4} = \frac{b_b - b_a}{m_a - m_b}, \qquad y_{P4} = m_b x_{P4} + b_b, \qquad \theta_{P4} = \arctan\frac{y_{P4}}{x_{P4}}. \tag{72}$$

Also:

$$R_4 = \sqrt{(x_{P4} - x_{04})^2 + (y_{P4} - y_{04})^2}. \tag{73}$$

The Cartesian equation of each arc is:

$$(x - x_{0i})^2 + (y - y_{0i})^2 = R_i^2, \quad i = 1, 2, 4. \tag{74}$$

Converting the previous equation, and using the appropriate sign for the radical in each case, yields the polar equations of each arc:

$$r_{12}(\theta) = x_{01} \cos\theta + y_{01} \sin\theta - \sqrt{(x_{01} \cos\theta + y_{01} \sin\theta)^2 - (x_{01}^2 + y_{01}^2 - R_1^2)},$$

$$r_{23}(\theta) = x_{02} \cos\theta + y_{02} \sin\theta - \sqrt{(x_{02} \cos\theta + y_{02} \sin\theta)^2 - (x_{02}^2 + y_{02}^2 - R_2^2)}, \tag{75}$$

$$r_{45}(\theta) = x_{04} \cos\theta + y_{04} \sin\theta + \sqrt{(x_{04} \cos\theta + y_{04} \sin\theta)^2 - (x_{04}^2 + y_{04}^2 - R_4^2)}.$$

The Cartesian equation for the straight line $P_3 P_4$ is:

$$y = m_a x + b_a. \tag{76}$$

Converting to polar coordinates:

$$r_{34}(\theta) = \frac{b_a}{\sin\theta - m_a \cos\theta}. \tag{77}$$

By use of the concatenation procedure (6) the equation representing one half of the sprocket tooth is obtained:

$$r_{HT}(\theta) = r_{12}(\theta) + H(\theta, \theta_{P2})\{-r_{12}(\theta) + r_{23}(\theta)\} + H(\theta, \theta_{P3})\{-r_{23}(\theta) + r_{34}(\theta)\}$$
$$+ H(\theta, \theta_{P4})\{-r_{34}(\theta) + r_{45}(\theta)\}. \tag{78}$$

The equation of the full sprocket toothed contour is obtained by simply replacing θ by the reflecting and repeating function, $R(N, \theta)$:

$$r_T(N, \theta) = r_{12}\big(R(N, \theta)\big) + H\big(R(N, \theta), \theta_{P2}\big)\{-r_{12}\big(R(N, \theta)\big) + r_{23}\big(R(N, \theta)\big)\}$$
$$+ H\big(R(N, \theta), \theta_{P3}\big)\{-r_{23}\big(R(N, \theta)\big) + r_{34}\big(R(N, \theta)\big)\}$$
$$+ H\big(R(N, \theta), \theta_{P4}\big)\{-r_{34}\big(R(N, \theta)\big) + r_{45}\big(R(N, \theta)\big)\}. \tag{79}$$

It is pertinent to point out that (78) was established resorting to concatenation procedure (6) and not (7) because the subsequent insertion of $R(N, \theta)$ instead of θ in (79) automatically limits the half tooth, to be reflected and repeated, to the angle starting at $\theta = 0$ and ending at $\theta = T/2 = \pi/N$.

4.2.2. Hub

The equation for the hub contour is simply:

$$r_H = \frac{D_H}{2} \tag{80}$$

and the extreme points of the hub contour are considered to be:

$$\theta_{P6} = 2\pi, \qquad \theta_{P7} = 4\pi. \tag{81}$$

4.2.3. Bore and keyway

Fig. 14 shows the top half of both the keyway and the bore. The coordinates of points P_8, P_9 and P_{10} are as follows (in a sequence appropriate for numerical evaluation):

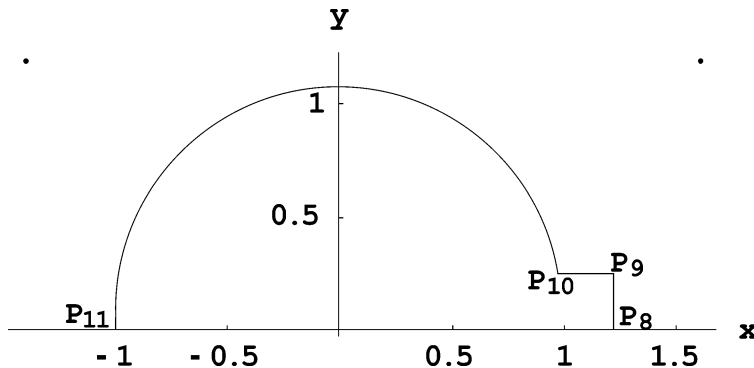$$\psi_{P10} = \arcsin\frac{k}{D_B},$$

Fig. 14. One half of the bore and keyway, plot of Eq. (84).

$$x_{P10} = \frac{D_B}{2}\cos\psi_{P10}, \qquad y_{P10} = \frac{k}{2}, \qquad \theta_{P10} = 4\pi + \psi_{P10},$$

$$x_{P8} = \frac{D_B}{2}\cos\psi_{P10} + \frac{k}{2}, \qquad y_{P8} = 0, \qquad \psi_{P8} = 0, \qquad \theta_{P8} = 4\pi + \psi_{P8}, \tag{82}$$

$$x_{P9} = \frac{D_B}{2}\cos\psi_{P10} + \frac{k}{2}, \qquad y_{P9} = \frac{k}{2}, \qquad \psi_{P9} = \arctan\frac{y_{P9}}{x_{P9}}, \qquad \theta_{P9} = 4\pi + \psi_{P9}.$$

The equations of the curves that make up one half of the keyway and the bore, Fig. 14 are:

$$r_{89} = \frac{x_{P8}}{\cos\theta}, \qquad r_{9,10} = \frac{y_{P9}}{\sin\theta}, \qquad r_{10,11} = \frac{D_B}{2}. \tag{83}$$

Concatenating these equations yields the equation for one half of the bore and the keyway:

$$r_{HBK} = r_{8,11}(\theta) = r_{89} + H(\theta, \theta_{P9})(-r_{89} + r_{9,10}) + H(\theta, \theta_{P10})(-r_{9,10} + r_{10,11}). \tag{84}$$

To obtain the full bore and keyway equation θ is now replaced by the reflect and repeat function which for $N = 1$ now simply reflects and does not repeat:

$$r_{BK} = r_{8,11}\big(R(\theta, 1)\big). \tag{85}$$

4.2.4. General equation of the sprocket

Thus the general equation for the main (side) view of the sprocket including the toothed contour, the hub, the bore and the keyway is:

$$r = r_T + H(\theta, 2\pi)(-r_T + r_H) + H(\theta, 4\pi)(-r_H + r_{BK}) + H(\theta, 6\pi)(-r_{BK}). \tag{86}$$

4.3. Example: a specific sprocket

Consider an ASA, No. 80 sprocket, i.e., $1''$ (0.0254 m) pitch with 13 teeth:

$$P = 1'' \quad (0.0254\text{ m}), \qquad N = 13, \tag{87}$$

which according to (Oberg et al., 1988; Dodge Engineering Catalog, 1993), have the following values for the roller diameter and the hub diameter:

$$d = 0.625'' \quad (0.0159\text{ m}), \qquad D_H = 3'' \quad (0.0762\text{ m}), \tag{88}$$

choosing the maximum permissible bore diameter, Dodge Engineering Catalog, and an adequate size of square key:

$$D_B = 2'' \quad (0.0508\text{ m}), \qquad k = 0.5'' \quad (0.0127\text{ m}). \tag{89}$$

Substituting values (87)–(89) into Eqs. (68)–(86) converts the general equation of the sprocket (86) into the equation of this specific sprocket. Fig. 15 is a direct plot of this specialized equation.

5. Conclusions

A methodology, referring to an extension of Analytic Geometry, has been presented by which finite segments of lines and curves may be represented by equations without requiring any inequalities. Also, it has been illustrated how any number of these finite segments may be concatenated into a single curve
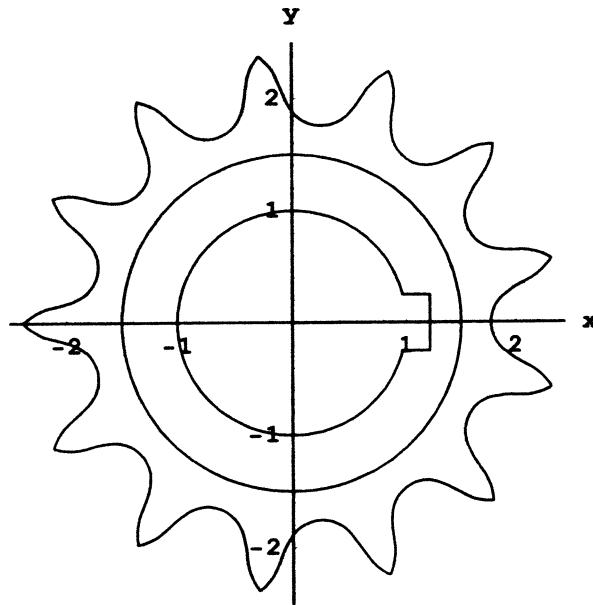
Fig. 15. Sprocket, plot of Eq. (86) for values (87)–(89).

represented by a single equation valid from $-\infty$ to $+\infty$. The curves may be open, closed, with or without polar symmetry. The general equation of a polygon and even that of the chain sprocket have been established, the latter including toothed profile, hub, bore and keyway.

This has been accomplished by use of algebraic and transcendental functions exclusively. The scheme is simple and straightforward and its use merely requires a working knowledge of Analytic Geometry.

References

Chicurel-Uziel, E., 1999/2000. Non-piecewise representation of discontinuous functions and its application to the Clebsch method for beam deflections. Meccanica 34 (4), 281–285.

Chicurel-Uziel, E., 2000. Closed-form solution for response of linear systems subject to periodic, non-harmonic excitation. J. Multi-Body Dynamics Proc. Inst. Mech. Engrs. 214 (K3), 189–193.

Chicurel-Uziel, E., 2001a. Exact, single equation, closed form solution of vibrating systems with piecewise linear springs. J. Sound Vibration 245 (2), 285–301.

Chicurel-Uziel, E., 2001b. Exact, no transform solution of multi degree-of-freedom vibrations with non-harmonic, periodic excitation. J. Multi-Body Dynamics Proc. Inst. Mech. Engrs. 215 (K3), 163–169.

De Berg, M., et al., 1998. Computational Geometry, Algorithms and Applications, 2nd Edn. Springer.

Drakopoulos, A., Örnek, E., 2000. Use of vehicle collected data to calculate existing roadway geometry. J. Transportation Engineering 126 (2), 154–160.

Dodge Engineering Catalog, 1993. Reliance Electric, 1.1R, p. D11-24.

Hakimi, S.L., Schmeichel, E.F., 1991. Fitting polygonal functions to a set of points in the plane. Graphical Model Image Processing 53 (2), 132–136.

Milenkovic, V., 1993. Robust polygon modeling. Computer-Aided Design 25 (9), 546–566.

Oberg, E., et al., 1988. Machinery's Handbook, 23rd Edn. Industrial Press 2301.

Preparata, F.P., Shamos, M.I., 1985. Computational Geometry, An Introduction. Springer-Verlag, pp. 271–311.

Wolfram, S., 1996. The Mathematica Book, 3rd Edn. Cambridge University Press.